2.9 Storage Ring Injection

2.9.1 Overview

The Storage Ring injection requires five magnet systems:

Kicker K1
Kicker K2
Kicker K3
Kicker K4
Septum Y12

An overview of the equipment placement is shown in Fig.f291_a. Fig.f291_b shows the general layout of the Storage Ring injection magnets in the machine tunnel. These magnet systems are summarised in Tables t291_a and t291_b.

Magnet Technology	Metallised ceramic chamber, with conductor and ferrite core in air
Magnet Deflection	4.5mrad
Circulating Beam Aperture	+/-45mm (H) x 40mm (V)
Magnet Length	600mm
Magnet Field	65mT
Magnet Inductance	≈1.3μH
Magnet Current	2.5kA
Magnet Current Waveform	Over-damped half-sine, around 6μs length
Total Non-Systematic Error	<1.0% horizontal, 34μrad vertical

Table t291_a: Summary of Storage Ring Kickers K1-K4.

Magnet Technology	Eddy current, with electron beam chamber and magnetic screen
Magnet Deflection	5.0^o
Circulating Beam Aperture	+45/-18mm (H) x 24mm (V)
Injected Beam Aperture	25mm (H) x 6mm (V)
Magnet Length	800mm
Septum Thickness	3mm
Magnetic Field	0.87T
Leakage Deflection	0.01% horizontal, 6μrad vertical
Magnet Inductance	4.0μH
Magnet Current	4.2kA
Magnet Current Waveform	Single-cycle sine, 120μs duration
Total Non-Systematic Error	<0.6% horizontal, 430μrad vertical

Table t291_b: Summary of Storage Ring Septum **Y12**.

The Storage Ring kickers are operated at identical currents to give a symmetric 15mm bump to the stored electron beam. The septum **Y12** is similar to the Booster septa Yi and Ye. The septum magnets use an improved eddy current design, with preliminary measurements indicating a peak leakage field below 0.01%.

Initial investigation (Ref.4) showed that top-up injection into the Storage Ring was not possible without giving a small disturbance to the beam-line experiments; the approach taken is to provide additional timing pulses to experiments which permit a momentary pause in data acquisition, if required.

The error tolerances are under continuing study (Ref 1-5). The error estimates given in the above Tables are worst-case values for these magnet systems; typical operational values should be much less.

Several possibilities for placement of the kickers and septum in the long straight were investigated, giving rather similar deflection requirements; the placement of **Y12** shown in Fig.f291_b is found by minimising the kicker deflection while still permitting passage of Transfer Line 2 past the kicker K2.

2.9.2 Kicker Technology

The whole aspect of kicker technology was re-evaluated (Ref.6 - 55). The use of semiconductor switches is attractive to avoid on-going maintenance of thyratrons, and also to reduce equipment cost.

The possibility of using a slotted line kicker (Ref.13 - 15) was seriously considered for the Storage Ring. However, to maximise the use of the Storage Ring, nearly complete filling pattern is needed. In this case, the injection bump must give a perfectly smooth time transition. In particular, it is vital to match the transverse fields of the inner two magnets K2 and K3. A metallised ceramic chamber is much better than the slotted line magnet in this respect. Regrettably, the metallised ceramic chambers are also a much more expensive technology.

2.9.3 Kickers K1-K4

The ideal is to have four identical kickers with field waveforms that track each other in time to permit top-up injection with small perturbation of the stored electron beam. A reasonable effort is to be put towards minimising tracking error, so that the duration of the stored beam disturbance is minimised. The pulsed power supplies and magnets would feature precise temperature control. Each magnet is fitted with a flashing warning light and interlock switches over the access hatches, for personnel safety.

Experience indicates that unexpected overheating of the ceramic chamber by the circulating electron beam is a problem. For the SLS, the external magnetic field pulse is a relatively slow half-sine pulse; eddy current losses can be high, since the requirement is only that the four kickers give identical magnetic field pulses. The resistivity for the metallisation is 0.15Ω/square +/-20%; this would give losses in the ceramic of <10W, not counting the resistive loss due to the RF contact fingers. An even lower value of resistance is not advisable because the uniformity of the metallisation is not so high; in turn, this means that the large eddy current attenuation of the kicker field would be different in each chamber. The metallisation thickness would be equated to the surface roughness of the ceramic.

Overheating is still a concern, so these magnets should be designed to permit forced air cooling. This means that an "H-frame design" is preferred over a "window-frame design", since there is space for cooling air. The conductors are held in place with precise machined insulating plates, and the ferrite with high conductivity contact strips.

The field homogeneity is good because of the large vertical gap, but the homogeneity risks being limited by non-uniformity of the metallisation. The coil voltages are low, and the choice is made to have no conductor encapsulation.

The vertical beta-function in the injection straight is normally below 10m, while the maximum in the Storage Ring (where the standard chamber height is 35mm) is about 22m. Thus the vertical aperture could be reduced to 35mm x 10/22 = 14.5mm. However, with this reduced aperture, the electron beam image current would be concentrated on a very narrow strip of the metallisation. As an engineering compromise, a ceramic chamber height of 28mm is chosen, giving +/- 6.75mm clearance for chamber dimension errors, RF finger contacts and chamber alignment errors. In turn, this gives a reasonable magnet current of about 2kA.

The window-frame magnet design with a metallised ceramic chamber is is shown in Fig.f293_a. The outer edge of the ceramic chamber has 10mm X-ray clearance.

A circuit for the pulser is shown in Fig.f293_b. An SCR switch is shown, but this could also be a thyratron. The switch requires 10-20μsec to turn off, so to prevent reverse current flowing, all the energy is discharged. The circuit shows two diode discharge paths. The discharge resistances are low value, and would be implemented with precision coaxial rods of resistive metal; this type of resistance would be very stable. The simulation result is in Fig.f293_c. The current rise is quasi-sinusoidal, and the fall is quasi-exponential. The total pulse length is greater than the required value of 6μsec, but the long discharge tail should be highly reproducible. Circuit improvements are being investigated.

2.9.4 Septum Technology

The choice was made to use a common design for all of the septum magnets and their vacuum tanks, to reduce design effort. Ref.1 gives a pulse length for a given flat-top accuracy, and this optimum value is around 70μsec. A survey of previous septum designs showed that a peak leakage field of 0.06% was typical, except for Eddy Current designs where the values were around 1%.

The advantages of an Eddy Current design are:

- simpler magnet - less cost for construction;
- reduced risk of insulation failure;
- curved magnet giving monotonic decrease of stray field away from region of septum exit (rectangular block construction typical for Front-Leg design gives peak stray fields at both ends);
- low electron beam impedance is easily achieved;
- septum presents no cooling problem.

The advantages of Front-Leg design:

- stray field appears only during current pulse (diffusion current in an Eddy Current design lasts several hundred microseconds afterwards);
- stray field might be much less than for an Eddy Current design, but this is dependant upon design and assembly tolerances;
- current pulse length could be increased if really necessary, for improved current measurement accuracy.

There are reported large improvements in leakage field for both Front Leg (Ref 60) and Eddy Current (Ref 56) designs by adding a low permeability electron beam chamber. The choice for SLS is an eddy current design; to reduce the risk to the project, a prototype eddy current magnet incorporating a magnetic screen chamber was tested.

The short magnet pulses means that the energy dissipated in the magnet is around 10W. The worst case dissipation occurs if a full energy beam from the booster is lost at the 3Hz rate on the septum conductor; this amounts to 0.01A x 2.4GeV x 3Hz x 700nsec, or 50W. The cooling channels are placed as close as possible to the septum for this reason. The water flow is given by

$$Flow(kg/s) = \frac{P}{\kappa.\Delta T},$$

where κ is the specific thermal capacity of water, 4174J/kg^{o}C. The water flow is set to have a flow that is reliably measured; a value of 0.05L/s is chosen, giving a negligible temperature rise in normal operating conditions.

The septum magnets will be housed in similar vacuum chambers. Fig. f294_a and f294_b show a typical tank. The ribs inside the tank are machined flat after welding to give the required horizontal mechanical tolerances. Precision locating holes are drilled into these ribs, and also on the top surface of the tank to give on-axis alignment points. The easy top access to the rectangular tank is an important feature to avoid assembly difficulties. The pulsed power supply is mounted directly beside the tank, and features a thermostatically-controlled cooling fan to maintain the capacitors at a constant temperature. Each tank is fitted with a flashing warning light and interlock switches over the access hatches, for personnel safety.

2.9.5 Septum Y12

The septum Y12 has a electron beam chamber added to the eddy current septum to present a continuous profile to the circulating beam. This chamber is made from 0.5mm stainless steel. The outgassing surface of the 0.2mm magnet laminations is large - perhaps 60m^2 - which is comparable to the entire vacuum surface of the rest of the Storage Ring. The stainless steel chamber has the secondary purpose of giving a very low gas conductance from the laminations to the circulating electron beam. Two large (500L/s) pumps are installed on the Transfer Line side to maintain a reasonably low gas pressure, $<10^{-8}$ mbar, and the Storage Ring gas pressure should remain $<10^{-9}$ mbar.

The provisional choice is made to have Y12 without any mechanical translation in the horizontal plane. Any experiments concerning the septum placement can be implemented with four DC magnets, powered in series, to give an additional bump in the long straight section. In the distant future, it may be possible to use a small transient currents, generated by a DSP card, to correct the residual errors in K1-K4.

The vertical injected beam clearance required is estimated solely from gross beam steering errors during commissioning at 6mm. The horizontal injected beam clearance of 25mm is not required for injected beam clearance, but gives an inductance which is reasonably large with respect to stray inductances.

The basic pulser circuit for all the septa is shown in Fig.f295_b; the magnet and capacitor values are indicative only. The relevant stray inductances, resistances and capacitances are included. Experimentation with the prototype septum showed that the leakage field could be greatly reduced by using a bipolar current pulse, not unipolar. In addition, no extra work was required to build a pulser which gave a bipolar pulse.

In Fig.f295_b, the capacitor C1 is charged from a 1.2kV / 0.01A constant current supply; a charging switch U1 is shown to isolate the charging supply from the discharge transient. The SCR X1 discharges the capacitor through the magnet L2. After the current has passed the maximum value, the capacitor becomes negative with respect to ground, and the recharging current starts to flow through D1 and D2. This gives a 50µs interval for the SCR recovery. However, D1 and D2 then have a turn-off transient, so the modest snubber network C4 / R7 / L8 limits the dV/dt across the SCR to give a safety margin against re-triggering. The measured values for the important inductance between the SCR and D1/D2 are exceptionally small, but the mesured results in Fig.f295 c confirm these. The capacitor voltage before and after the pulse indicate the energy loss, using

$$E_{\max} = \frac{CV^2}{2}$$

For the 4kA pulse in Fig.f295 c, the energy before the pulse was 19.7J and after 13.1J. Thus each pulse dissipates only 6.6J in the entire circuit, i.e 20W for 3Hz operation. About half of this loss is in pulser, not the magnet.

The control circuit for these supplies is relatively simple, and will be modeled on the ESRF design (Ref 72). Features of the pulse power supplies are:

- two independent current transformers, one for regulation and one for Control Room monitoring;
- a SCR gate driver with sub-microsecond accuracy;
- a timing circuit which fixes the trigger-to-peak current time delay;
- temperature stabilisation for the discharge capacitors;
- physically small pulser mounted in the machine tunnel;

2.9.6 References and Bibliography

SLS Development

1. “Error Tolerances of Half-Sine Pulses”, CH Gough, SLS Note 2/97, Jan 97
2. “Comparison of Pulsed Power Supplies for Kicker Magnets”, CH Gough, SLS Note 12/97, Jun 97
3. "Error Estimates of Injection Magnets", CH Gough and A Streun, SLS Note 16/97, Oct 97
4. "Tune Limits with the Storage Ring Septum Magnet", CH Gough, SLS Note 19/97
5. "Error Allocations for the SLS Pulsed Magnets", C H Gough, SLS Note 20/97

Ceramic Chambers

6. "On the Resistive Coating of the Kicker Ceramic Chamber", E Karantzoulis, Sincrotrone Trieste ST/M-TN-92/1, Feb 92
7. "Using a Ceramic Chamber in Kicker Magnets", S Kurennoy, PAC93, p3420-2
8. “Study on the metallic coating of the ceramic chamber for the ATF damping ring kicker magnets”, Terunuma-N; Nakayama-H; Urakawa-J, PAC95, p1906-8
9. "Deposition of Metallic RF Shield Stripes in Long Ceramic Beam Chambers", Hodges T et al, 15th International Conf. on High Energy Acclerators, Hamburg 1992, p356-8
10. "Surface Resistivity Tailoring of Ceramic Accelerator Components", Anders S et al, PAC 93, p.1390-2
11. "Metallized Ceramic Vacuum Chambers for the LEP Injection Kicker Magnets", Mayer M et al, EPAC88, P.1378-80
12. "Calculation of Magnetic Field Attenuation by Metalized Coating and Core Material for Pulsed Magnet", S Matsui et al, 8th Symp. on Acclerator Science and Technology, 1991 Saitama Japan, p217-9

Finger Contacts

13. "Design Studies on a Vacuum Bellows Assembly with Radio Frequency Shield for the KEK B Factory", Suetsugu Y et al, Rev. Sci. Instr. 67(8), Aug 96
14. "Impedance Measurements of Components for the ALS", Corlett JN et al, PAC93, p.3411-3

Kickers without Magnetic Material

15. "A Slotted-Pipe Kicker for High-Current Storage Rings", G Blokesch et al, Nuclear Instruments and Methods in Physics Research A 338 (1994) p151-5
16. Impedance Study for a Slotted-Pipe Kicker Magnet", Z Feng, EPAC96, p1311-3
17. "Eddy Currents Induced in a Muon Storage Ring Vacuum Chamber due to a Fast Kicker", WQ Feng et al, PAC95 p1257-9
18. “New Injection Kicker Magnets for the Daresbury SRS”, Clarke JA et al, PAC pp1469-71
19. “The Operation of Injection Kickers in the SRS”, Bradshaw DJ et al, EPAC94, pp2400-2

20. “DAΦNE Accumulator Kickers”, De Simone S et al, EPAC92 p1449-51
21. "The Los Alamos Proton Storage Ring Fast-Extraction Kicker System", JF Power et al, p3021-3, IEEE Trans Nucl.Sci., Vol NS32 No5, October 1985

Kickers with Magnetic Material

22. “Kicker Magnets for the Advanced Light Source”, Gabor et al, PAC89,
23. “Test Results of the 8.35kA, 15kV, 10pps Pulser Prototype of the ELETTRA Kickers”, Fabris R et al, Sincrotrone Trieste Note ST/M-92/12
24. “Performance of the Elettra Injection System”, Fabris R et al, EPAC94, pp2355-2357
25. “The ELETTRA Fast Magnets”, Tommasini D et al, EPAC92, pp1452-4
26. “High Current, High Voltage Pulser for the ELETTRA Kicker Magnets”, Tommasini D et al, EPAC92 ,pp1606-8
27. “Magnetic Performance of Injection Bump Magnet for the SPring-8 Storage Ring”, Kumagai K et al, IEEE Trans. Magn. Vol 32, No 4, July 1996
28. "SLC Kicker Magnet Limitations", R Cassel et al, PAC91 p996-8
29. "Operational Experience with SLC Damping Ring Kicker Magnets, T Mattison et al, PAC91,p2331-3
30. "Fast and Reliable Kicker Magnets for the SLC Damping Rings", TS Mattison et al, PAC95
31. “Design and Testing of a High Voltage Coil for the Kicker Magnets of CERN’s Large Hadron Collider”, Mayer M et al, IEEE Electrical Insulation Magazine, Nov/Dec 96
32. “Beam Impedance of Ferrite Kicker Magnets, F Voelker et al, PAC89, p851-3
33. "Beam Induced Heating of Ferrite Magnets", WK van Asselt et al, PAC91,p881-3
34. “Application of Fibre Optic Magnetic-Field Sensor to Kicker Magnet”, Takada H et al, J Phys. E:Sci Instrum. (1988) 371-374
35. "Development of a Modular and Upgradeable Fast Kicker Magnet System for the Duke Storage Ring", RJ Sachtschale et al, PAC95 p1248-50

Ferrite Materials for Accelerators

36. "Improving the Performance of Kicker Magnet Systems" MJ Barnes et al, 15th International Conf. on High Energy Accelerators, 1992, Hamburg, p191-201
37. "Effect of Saturating Ferrite on the Field in a Prototype Kicker Magnet", MJ Barnes et al, p2544-6
38. "Power Conditioning for Coil Launchers: Adaptation of Low di/dt Thyristors to Circuits with High di/dt Requirements", N Gordadia et al, 9th International Pulsed Power Conference, 1993, IEEE New Yorkp776-8
39. "Optimization of Speed-up Network Component Values for the 30Ω Resistively Terminated Prototype Kicker Magnet", MJ Barnes et al, PAC93 p1330-2
40. "A Precise High Field Injection Kicker Magnet for the Fermilab Tevatron", J Dinkel et al, 9th IEEE International Pulsed Power Conference, 1993, p894-6 (experience with ferrites)
41. “Development of a High Quality Kicker Magnet System”, Dinkel J et al, PAC93, p1357-9 (experience with ferrites)
41a "Comparison of Ferrite Materials for Pulse Applications", J Dinkel et al, 1993 9th Pulsed Power Conference, p300-3

Passive Components

42. "PSR Switchyard Kicker System Improvements", TW Hardek, PAC91 p872-874
43. "Energy Storage Capacitors: Aging and Diagnostic Approaches for Life Validation", WJ Sargent et al, IEEE Trans. Magnetics, Vol MAG33 No1, Jan 1997, p501-6,
44. "The Impact of High Energy Density Capacitors with Metallized Electrode in Large Capacitor Banks for Nuclear Fusion Applications", DW Larson et al, 9th IEEE International Pulsed Power Conference, p-735-8
45. "Kick Stability Analysis of the LHC Inflectors", MJ Barnes et al, EPAC96 p.2591-3

Switches

48. “Fast Transistor High Voltage Switches”, Product Catalog, Behlke Electronic GmbH, Frankfurt
49. “Design and Preliminary Results for a Fast Bipolar Resonant Discharge Pulser Using SCR Switches for Driving the Injection Bump Magnets at the ALS”, Stover G et al, PAC93 p1351-3
50. “Analysis and Design Modifications for Upgrade of Storage Ring Bump Pulse System Driving the Injection Bump Magnets at the ALS”, Stover GD, PAC95, p1254-6
51. "Fast TEM Kicker with MOSFET Solid State Driver", A Saab et al, PAC91 p3174-6
52. "Solid State Switch Application for the LHC Extraction Kicker Pulse Generator", E Vossenberg et al, Conference Record of the 1996 Twenty-Second International Power Modulator Symposium IEEE, p.67-70.
53. "SPICE Modelling of a FET-Switched Induction Accelerator Cell", CW Ollis et al, 9th IEEE International Pulsed Power Conference 1993, p.699-701
54. "Fast Switching Performance of Gate-Turn-Off Thyristor for Intense Pulsed-Power Supply", A Tokuchi et al, Nuclear Instruments and Methods in Research A 374 (1996), p352-8
55. "A mathematical model of a three-gap thyratron simulating turn-on", Barnes-MJ et al Digest of Technical Papers.Ninth IEEE International Pulsed Power Conference p.293-6

SPring-8 Septa

56. The Injection Septum Magnets of SPring-8 Storage Ring”, IEEE Trans. Mag, Vol 30 No 4, July 1994, p2134-2137
57. "Development of the Pulse Magnets for the Booster Synchrotron of SPring-8", H Yonehara et al, PAC95, p1358-60
58. "Field Measurement of a Pulsed Septum Magnet and R&D for SPring-8", K Kumagai et al, 8th Symp. Accelerator Science and Techn., 1991, Japan, p.220-222
59. "Study of the Injection Devices for the Storage Ring of SPring-8", H Miyade et al, 7th Symp. Accelerator Science and Techn., 1989, Japan, p.169-171

APS Septa

60. "The APS Direct-Drive Pulsed Septum Magnets" S Sheynin et al, PAC95 p.1355-7
61. "A Pulsed Septum Magnet for the APS", LR Turner et al, PAC93, p.2817-9
62. "The APS Thin Pulsed Septum Magnets", F Lopez et al, PAC95, p.2406-8
63. “Some Thought on an Eddy Current Septum Magnet”, K Halbach, APS/IN/MAG/94-1, 6 May 1994
64. "Circuit Description of the Power Systems for Pulsed Septum Magnets at APS", DG McGhee, PAC93, p914-6

Elettra Septa

65. "High Current Passive Septum Magnet for Elettra”, Fabris R et al, EPAC92, pp1460-2
66. “The Septum Magnets of Elettra” Fabris R et al, PAC93, pp1378-80
67. “Performance of the Elettra Injection System”, Fabris R et al, EPAC94, pp2355-2357
68. “Design, Construction and Testing of the Elettra Injection System”, Giannini M et al, EPAC94 2352-4

ESRF Septa

69. “Etude du Septum d’Injection S3 de l’Anneau de Stockage de ESRF (Type Classique)”, R Valbuena, CERN PS/PA-S Note 90-23, 3 juillet 1990
70. “Etude du Septum d’Injection S3 de l’Anneau de Stockage de ESRF”, R Valbuena, CERN PS/PA-S Note 90-14, 10 avril 1990
71. “Eddy Current Septum Magnet for the ESRF”, F Rohner, CERN Internal Note /AT/MA/90-08, 30 April 1990
72. "Redesign of Pulsed Power Supply Regulation Circuit", CH Gough ESRF Internal Note,17 Apr 94
73. "Design of Precision Comparator", CH Gough, ESRF Internal Note, 1 June 93

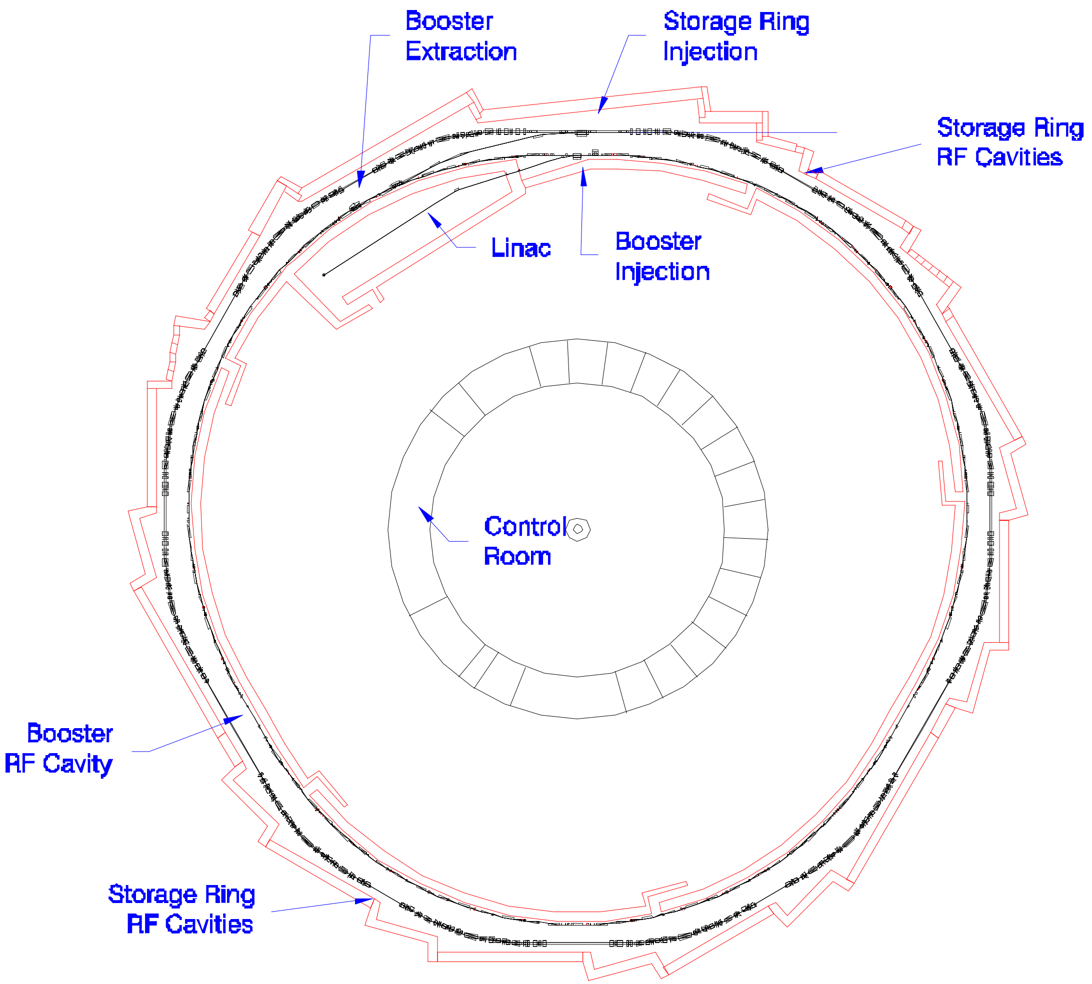

Figure f291_a:. General Placement of Equipment in the SLS

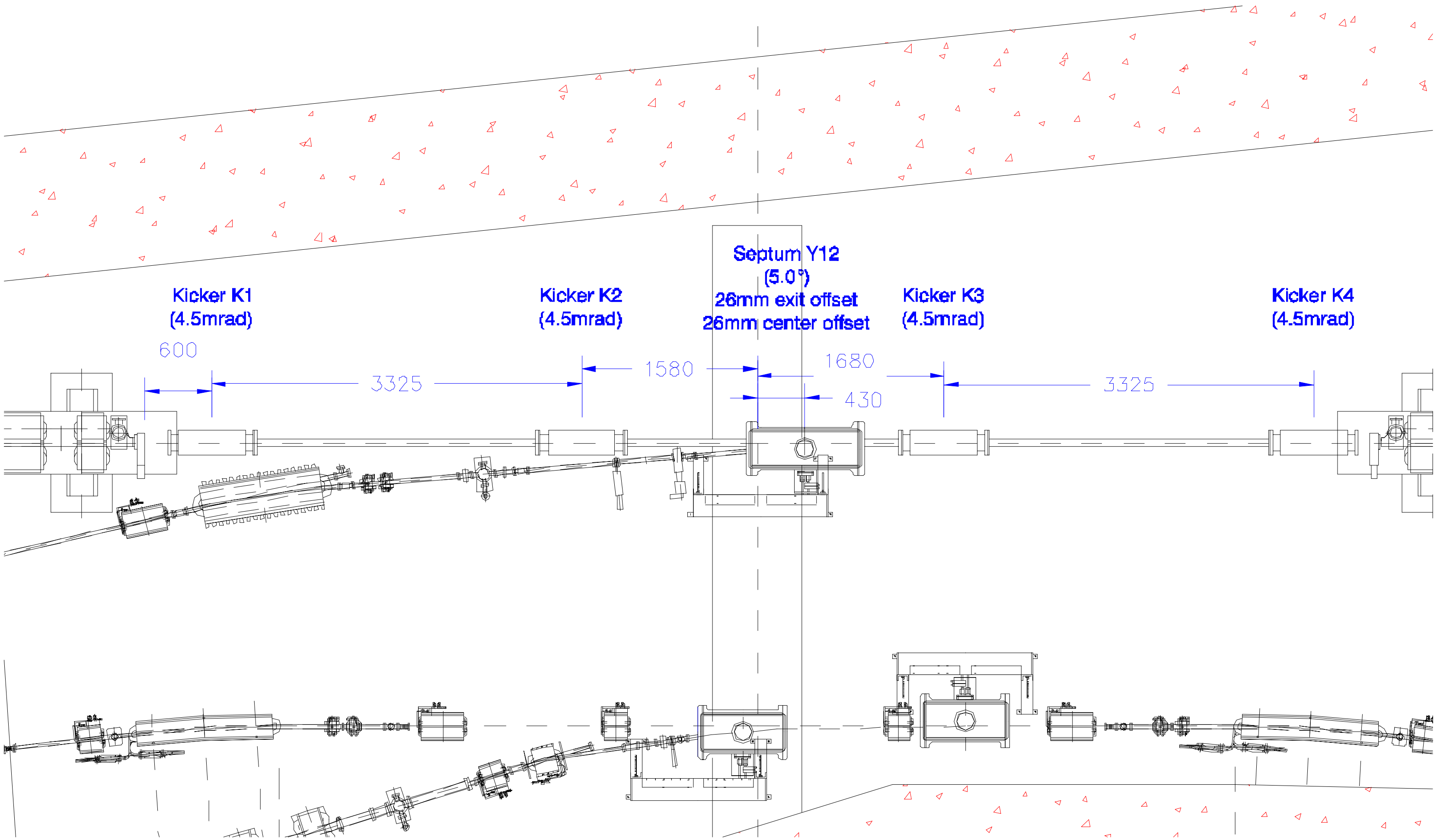

Fig.f291_b: Storage Ring injection configuration.

Kicker K2 (“H-Frame version”)

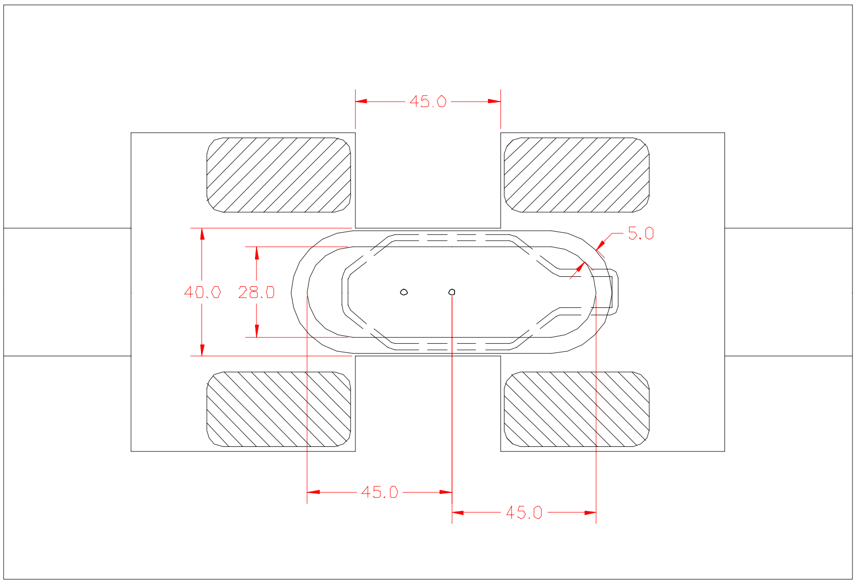

With LC Pulser

PARAMETER	GIVEN VALUE	DERIVED VALUE
Maximum Particle Energy E (GeV)	2.4 GeV	
Magnet Gap Length l (mm)	600 mm	
Angle (mrad)	4.5 mrad	
Bending Radius		133.33 m
Field Intensity		0.0600 T
Magnet Gap Width w (mm)	55 mm	
Magnet Gap Height g (mm)	40 mm	
Number of turns on magnet	1 turns	
Magnet Inductance		1.04 uH
Peak Current		1911 A
Energy in Magnet		1.9 J
Flat-top tolerance (+/-)	.1	
Particle Beam Duration (usec)	.7 usec	
Recommended Resonating Capacitor		4.6 uF
Recommended Capacitor Tolerance		28.5%
Recommended Half-Sine Pulse		6.9 usec
Go conductor X-section perimeter (mm)	50 mm	
Return conductor X-section perimeter(mm)	50 mm	
Resistive Loss per Cycle		21.2 mJ
Core Loss per Cycle		232.8 mJ
Pulse Repetition Rate (Hz)	3 Hz	
Power Loss		762.0 mW
Capacitor Voltage		935 V

Fig f293_a: Basic parameters for the Storage Ring kicker.
The dotted lines show the standard vacuum chamber cross-section.

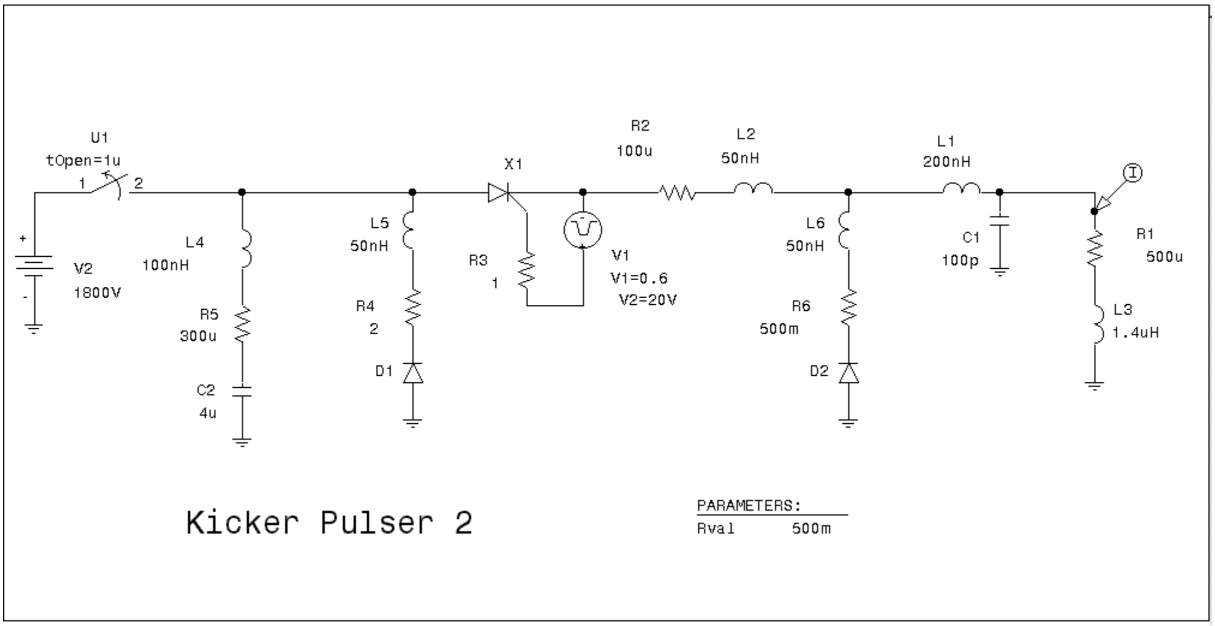

Fig f293_b: Pulser simulation circuit for Storage Ring kickers.
Component values are indicative only.

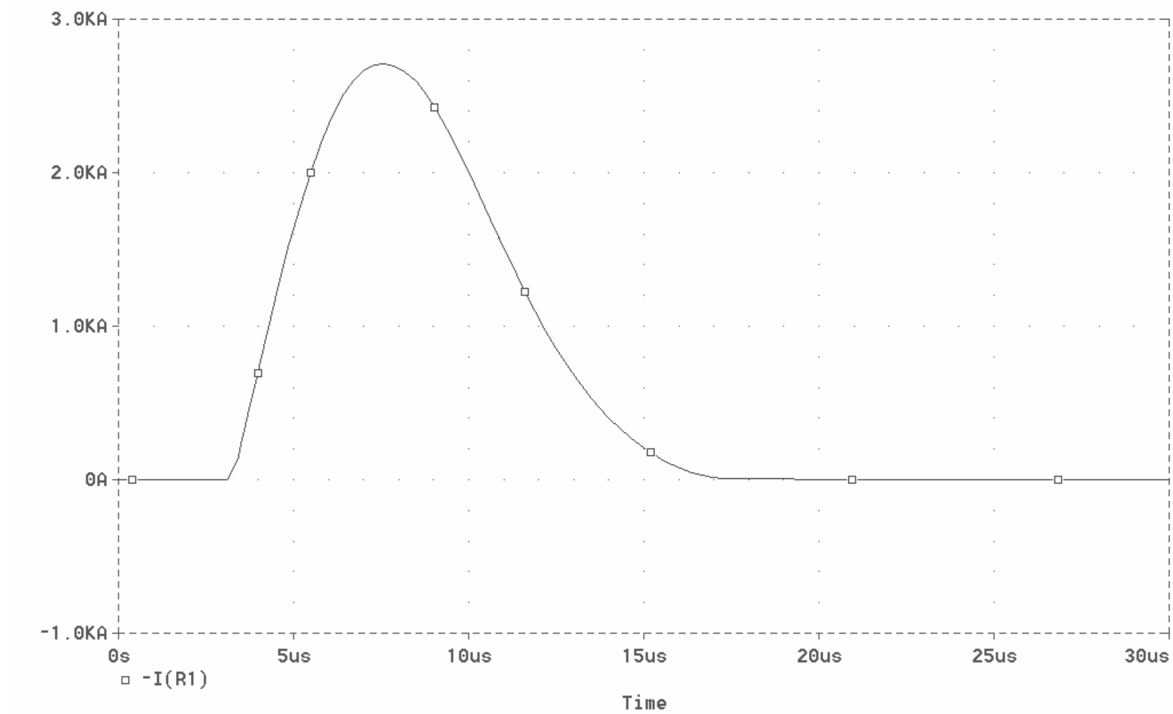

Fig f293_c: Simulation results for Fig f293_b

Storage Ring Septum

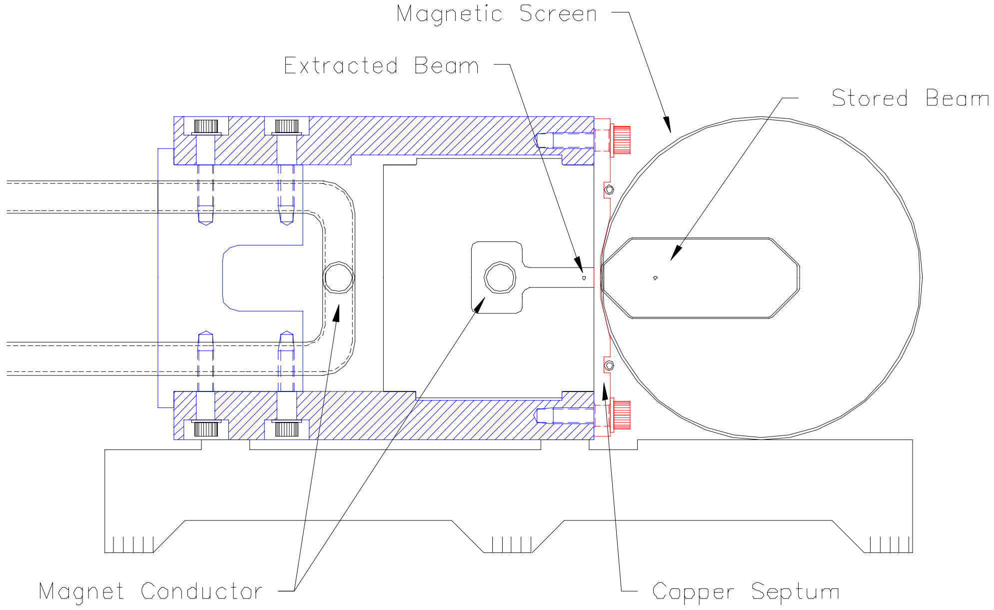

PARAMETER	GIVEN VALUE	DERIVED VALUE
Maximum Particle Energy E (GeV)	2.4 GeV	
Magnet Gap Length l (mm)	800 mm	
Angle (mrad)	87 mrad	
Bending Radius		9.20 m
Field Intensity		0.871 T
Magnet Gap Width w (mm)	25 mm	
Magnet Gap Height g (mm)	6 mm	
Number of turns on magnet	1 turns	
Magnet Inductance		4.19 uH
Peak Current		4157 A
Energy in Magnet		36.2 J
Flat-top tolerance (+/-)	.001	
Particle Beam Duration (usec)	.7 usec	
Recommended Resonating Capacitor		62.0 uF
Recommended Capacitor Tolerance		2.8%
Recommended Half-Sine Pulse		50.6 usec
Go conductor X-section perimeter (mm)	38 mm	
Return conductor X-section perimeter(mm)	38 mm	
Resistive Loss per Cycle		476.9 mJ
Core Loss per Cycle		6.6 J
Pulse Repetition Rate (Hz)	3 Hz	
Power Loss		21.4 W
Capacitor Voltage		1133 V

Fig.f295_a: View at EXIT of Storage Ring Septum, with magnet parameters.

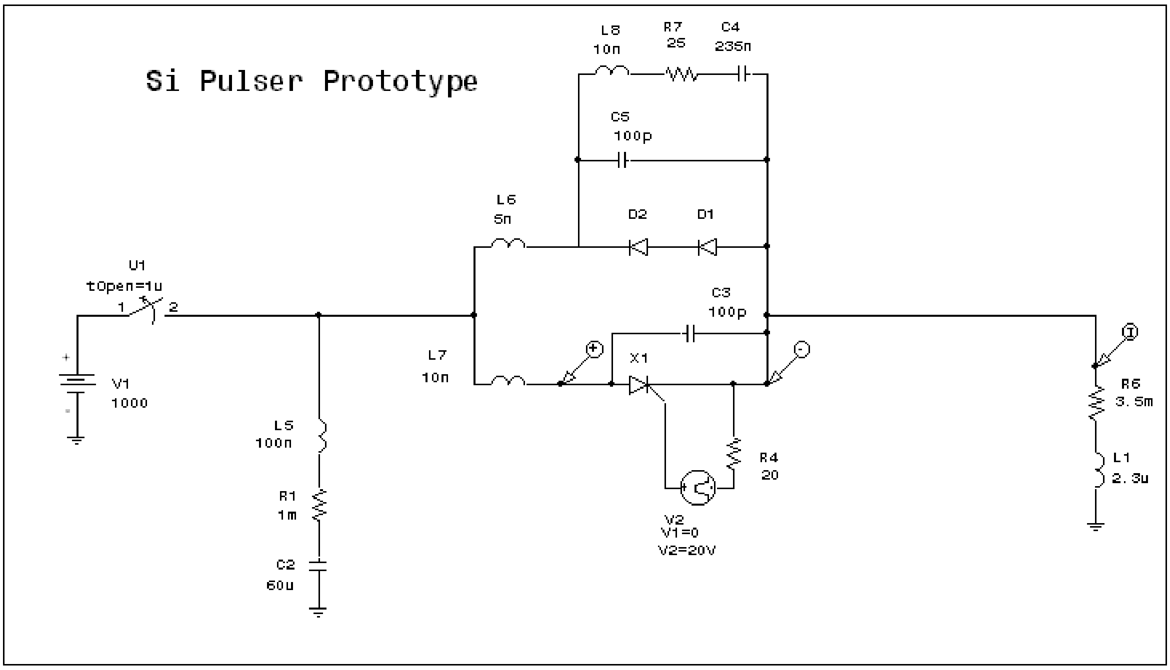

Fig.f295_b: Basic circuit for septum pulser for simulation.
The component values are indicative only.

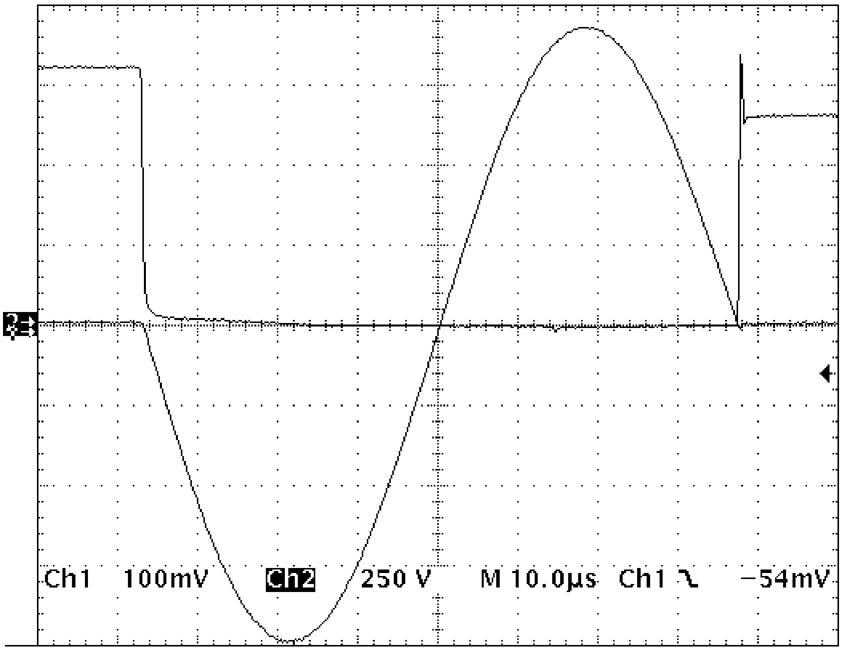

Fig.f295_c: Measured magnet current and switch voltage of the prototype pulser.

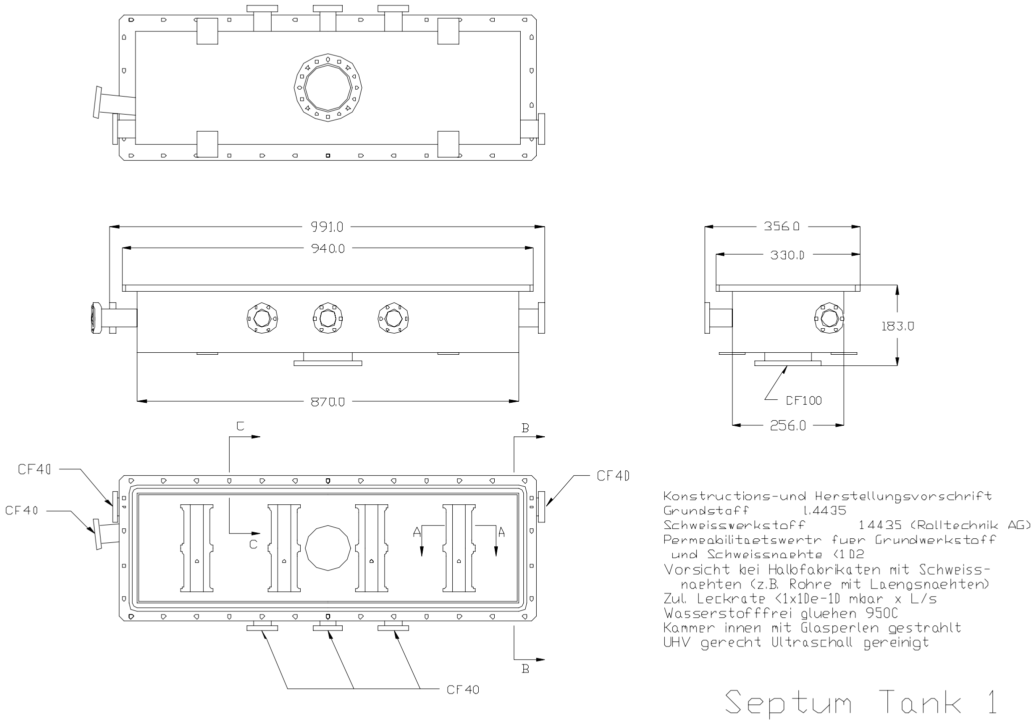

Fig f294_a: Typical vacuum tank for Septum Magnets

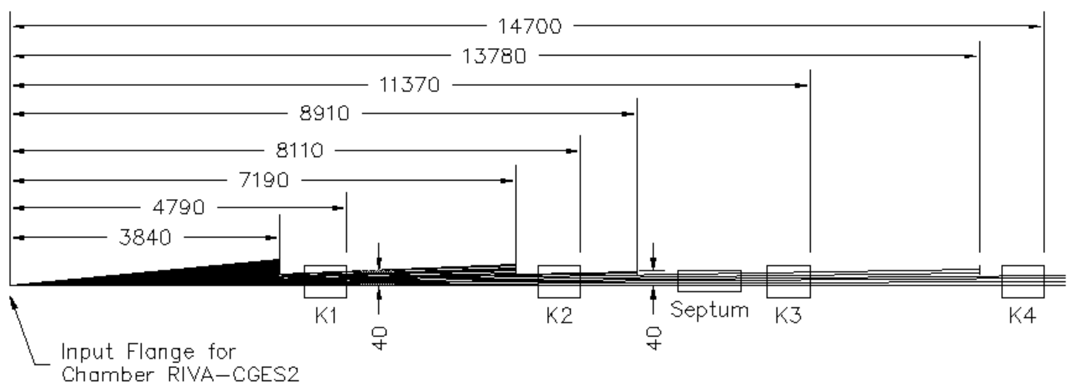

Fig f295: Ray-tracing to find minimum horizontal aperture of the vacuum chamber.
Four lumped absorbers are necessary to give reasonable aperture for the injection elements.